Unsaturated Liquid Percolation Flow through Nonwetted Packed Beds

D. Y. Liu, G. X. Wang, and J. D. Litster
Dept. of Chemical Engineering, The University of Queensland, Australia QLD 4072

The unsaturated flow of liquid through packed beds of large particles was studied using six different liquids, all with contact angles greater than 90° on the bed packing (wax spheres of 9, 15 and 19.4 mm diameter). The liquid flow was discrete in nature, as drops for low flow rates and rivulets for high flow rates. For unsaturated liquid flows, the actual percolation velocity, not superficial velocity, should be used to characterize the flow. The percolation velocity did not vary with packed-bed depth, but was a strong function of liquid flow rate, liquid and particle properties. Effects of liquid and particle properties (but not flow rate) are well captured by a simple correlation between the liquid–particle friction factor and Reynolds number based on actual percolation velocities. Liquid dispersion, characterized by the maximum dispersion angle, varies significantly with liquid and particle properties. The tentative correlation suggested here needs further validation for a wider range of conditions.

Introduction

When a liquid is introduced onto a packed bed of coarse particles, gravity-induced percolation occurs. This is a type of liquid flow commonly encountered in many chemical, geophysical, and metallurgical applications. Detailed understanding of this sort of liquid flow has been of concern, in particular, for numeric simulation of the chemical reaction, heat transfer, and mass transfer associated with the liquid percolation through packed beds.

It has been revealed experimentally that liquid percolation in packed beds might be either continuous or discrete (trickling) flow, depending on the properties of the liquid and packing particles, as well as certain process variables such as liquid flow rate and the existence of gas phase (Kolb et al., 1990; Melli et al., 1990; Rode et al., 1994). Many saturated liquid percolation examples can be classified as continuous flow, for example, filtration process of the liquid metals or alloys through a packed bed of refractory particles or ceramic foam filters (Apelian and Mutharasan, 1980; Frisvold et al., 1992). Extensive experimental and theoretical studies on continuous liquid flow have been carried out, leading to a number of models for simulation of such a flow in packed beds (Macdonald et al., 1979; Szekely and Kajiwara, 1979; Ohno and Kondo, 1980; Austin et al., 1997). These models are developed based on potential flow theory, so that their application to unsaturated liquid percolation is limited due to the discrete nature of the flow. The discrete nature of unsaturated liquid flow in packed beds has been identified experimentally using various photographic technologies, such as camera (Chew et al., 1997), X-ray (Gupta et al., 1996), microscope (Payatake et al., 1981), and high-speed video (Liu et al., 1997). For this reason, it is highly desirable to develop an alternative model to take the discrete nature of the unsaturated liquid percolation in packed beds into consideration.

To model the liquid distribution in trickle-bed reactors, a simulation algorithm has been proposed (Zimmerman and Ng, 1986), in which the gravity-induced liquid percolation was typically involved under an unsaturated flow condition. However, this algorithm needs a porous medium model that specifies the microscopic structure of the computer-generated packing, which does not seem to be applicable for the engineering-scale problems. Further study on the liquid dispersion in packed beds was carried out with a cold physical model, leading to a probability model based on the statistical motion of droplets (Ohno and Schneider, 1988). Similarly, the probability model also needs the information about the structure of the network formed by the particles and the lattice points in the intervals between the particles, making the

Correspondence concerning this article should be addressed to G. X. Wang.

model difficult to use. This model was later extended to estimate the flow region by combining with a potential flow model to simulate the liquid distribution (Wang et al., 1991). Such a treatment seems reasonable as a numerical technique, but this approach is conceptually problematic, because the discrete nature of the flow, as recognized by the probability model, is overlooked in the continuum-based simulation. There is another model available, referred to as the tube network dynamic model, in which the packed bed was simplified as a network of tubes with a constant inclination angle of 45° (Eto et al., 1993). However, it is still generally difficult to apply this model under the condition of discrete liquid flow through a packed bed, as the effective numerical calculation may have to be at the level of particle size.

As a matter of fact, the most important features for the unsaturated percolation in a packed bed are the interaction between the liquid and packing particles and the stochastic liquid motion due to the complex packing structure. Previous work (Wang et al., 1997a,b,c) paid particular attention to these characteristics of the flow, leading to an alternative liquid flow model, that is, force balance model with stochastic dispersion. For the moment, there is still further work to do for the general application of this model because the liquid–particle interaction and the stochastic motion have not yet been systematically investigated and formulated rigorously. Very limited experimental data are available for the unsaturated flow of nonwetting liquids through beds of large particles. Such systems, which allow discrete flow behavior, are important in a number of applications, particularly in the metallurgical industries.

In this work, a number of experiments have been performed to investigate the unsaturated percolation and the stochastic motion of discrete liquid flow through packed beds. These experiments will justify the applicability of a force-balance model under discrete liquid-flow conditions. The primary objective has been to quantify the interaction between liquid and packing particles and the liquid dispersion as the function of such liquid properties and packing characteristics as porosity of the bed and particle size. This study will provide a better understanding and practical formulations for modeling the unsaturated liquid flow through packed beds, based on experimental data.

Experimental Studies

Wax spheres were used as model particles. The wax spheres were made with Fish Ball Moulds from black wax purchased from Ajax Chemicals, of sizes 9 mm, 15 mm, and 19.4 mm. There was no significant deformation of such a packed bed under its own weight because all experimental runs were performed in cold conditions (temperature below 30°C).

Water and various solutions of glycerol, $CaCl_2$, and $ZnCl_2$ were employed in this study to investigate the effect of different liquids on percolation performance. All the liquids used have contact angles greater than 90° on wax. The properties of the liquids are listed in Table 1.

The experimental apparatus consisted of a packed column, two liquid tanks located on the top, and a liquid collector separately attached on the bottom of the packed column, as shown in Figure 1a. There are two types of liquid collector designed for the different measurements: an inverse-circular cone collector (Collector A) that was used to measure liquid percolation velocity, and an annular collector with four parts (Collector B) that was used to measure liquid radial distribution, as shown in Figure 1b. Note that the liquid was supplied from the tanks into the packed bed as a point source. The packed column, filled with the particles during experiments, was made from a 5-mm-thick Prespex sheet with an internal diameter of 282 mm and a height of 600 mm. The bottom of the packed column was supported by a metal mesh (4×4 mm) connected to the liquid collector. The height of the packed beds was designed so it could be adjusted from 100 mm to 500 mm when necessary.

During the experiments, the water head of the liquid tanks was kept constant. Two rotameters were employed to control the liquid flow rate at the initial and stable stages, respectively. A three-way valve was used to switch between the liquid supplies connected to the chosen rotameter (see Figure 1). Each experimental run was begun by (1) calibrating the rotameter; (2) starting from a dry bed, and (3) operating with a rotameter at an initial liquid flow rate that is 10% higher than the desired value until the steady-state condition for liquid flow was reached. The steady state for the unsaturated bed is the state at which the liquid flow rate introduced into the packed bed is approximately equal to the output flow rate of the liquid collected on the bottom of the packed bed under a steady gas flow. This was achieved by allowing liquid to flow through the packed bed for 15 min to stabilize the liquid holdup in the void space of the packing bed. After a steady flow condition was established, the liquid flow rate was set back to the desired value by switching the connection to another rotameter to perform the percolation, liquid distribution, and dispersion experiments.

Three types of measurements were made: percolation velocity, liquid distribution, and liquid dispersion.

Both the maximum and mean percolation velocities were measured. The maximum percolation velocity of liquid falling in the bed is defined by dividing the total height of the bed over the actual traveling time of the first representative liq-

Table 1. Properties of Liquids Used for Experiments

Liquid	Conc. (wt. %)	Density (kg/m^3)	Viscosity (kg/ms)	Surface Tension (kg/s^2)	Contact Angle on Wax (deg)
Water	—	1,000	0.0010	0.0732	105.6
0.5 glycerol	50	1,126	0.0060	0.0697	101.1
0.8 glycerol	80	1,209	0.0620	0.0676	96.6
0.85 glycerol	85	1,222	0.1130	0.0670	92.1
$CaCl_2$ solution	35	1,350	0.0059	0.0888	114.1
$ZnCl_2$	75	1,920	0.0340	0.0809	97.9

uid element moving from the top to the bottom of the bed. The mean percolation velocity is defined as the bed depth over the mean percolation time of the liquid flow at steady state. The mean percolation time is calculated by dividing the liquid flow rate by the liquid dynamic holdup in the packed bed. Liquid dynamic holdup was measured as the amount of liquid drained from the bed after suddenly shutting off the inlet flow valve, determined by weighing the collected liquid.

Liquid distribution at the base of the packed bed was measured in the following manner:

- The chosen liquid was sent through the packed column at the desired liquid flow rate from the top of the packed bed.
- Liquid was collected with the four annular collectors (see Figure 1b) after the flow was stabilized.
- The elapsed time was recorded and then the liquid in each collector was weighed, which allows determination of flux mass velocity for various collectors, giving liquid distribution.

The measurement of liquid dispersion focuses on the investigation of the percolation region due to the stochastic movement of the liquid in a packed bed. The region can be represented by the boundary of the liquid flow on the horizontal cross sections that was determined by measuring the liquid dispersion areas at different cross sections of the packed bed. A procedure similar to the liquid distribution experiments was employed for this measurement. A cotton sheet was placed on the metal mesh located on the bottom of the packed bed to record the wetted zone, and hence the dispersion area at each bed depth. The experimental measurements usually give the irregular dispersion areas, so an average dispersion radius was estimated by taking an average of eight dispersion radii, measured at equal angles around the central point of the bed.

Process Modeling

The visual experimental investigations previously performed have revealed that unsaturated percolation of liquid through packed beds is typically a discrete flow, especially if the liquid phase does not wet particles (Gupta et al., 1996; Liu et al., 1997). The liquid flows as droplets or rivulets over the bed packing. Experiments further reveal the existence of a major stream flow that is generally controlled by gravity. The liquid flow, along with a major stream (in the direction of gravity in this particular study), can be modeled by means

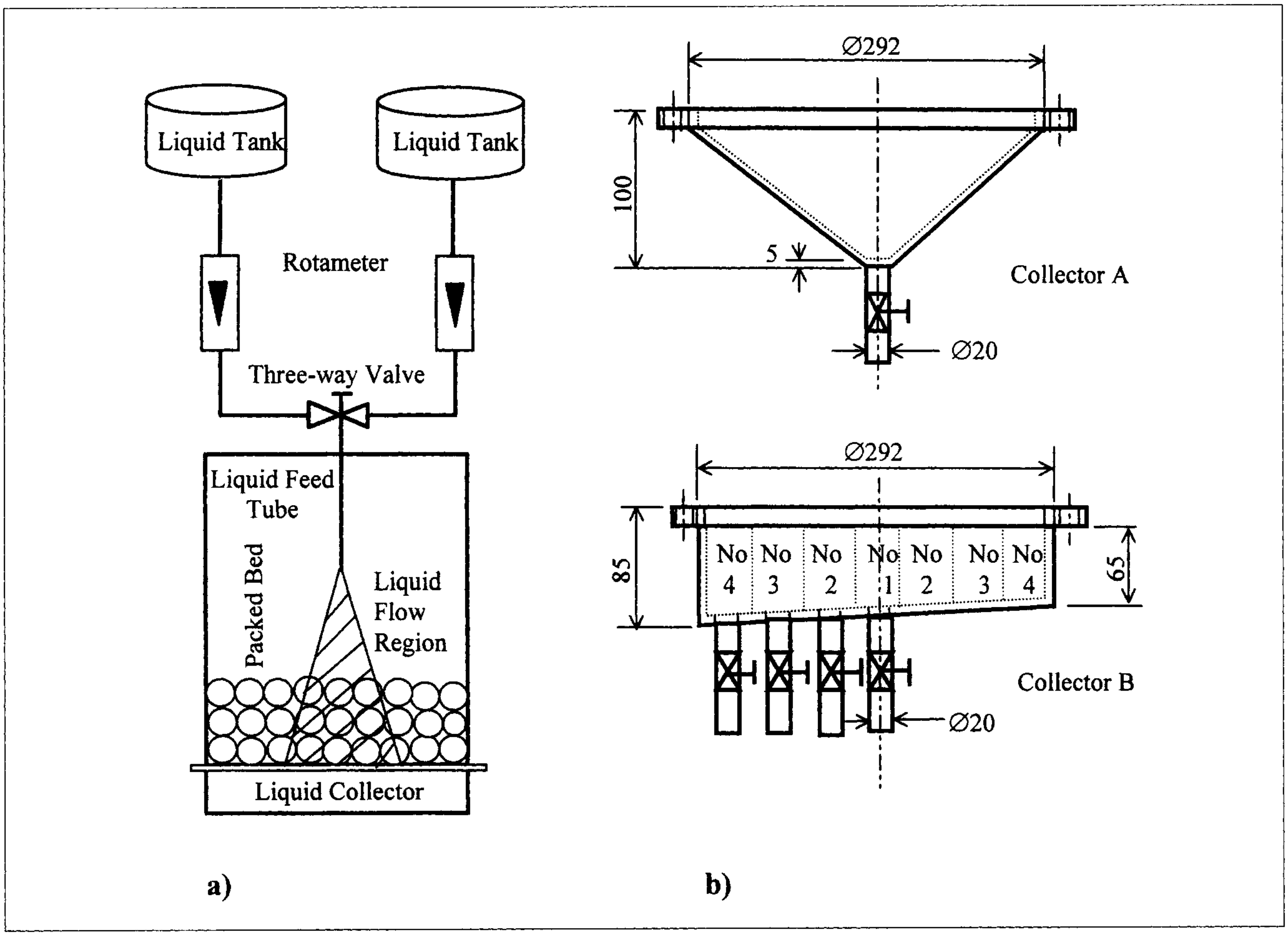

Figure 1. Experimental equipment.

(a) Experimental rig; (b) liquid collectors (unit: mm).

of the following force balance, that is

$$F_g + F_l^s = 0 \tag{1}$$

where F_g and F_l^s are the gravitational force of the liquid and the frictional force between the liquid and packed bed, respectively. These forces can be described as follows:

$$F_g = \rho_l g \tag{2}$$

$$F_l^s = \frac{C_{DS} a_{s-l}}{2} \rho_l |u_l| u_l \tag{3}$$

where ρ_l is the density of the liquid, kg/m^3; u_l is the percolation velocity of the liquid, m/s; g is the gravitational acceleration, m/s^2; a_{s-l} represents the specific liquid–particle contact area, l/m; and C_{DS} is defined as the liquid–particle friction factor.

The force balance concept has been employed to describe the discrete flow through a packed bed (Gupta et al., 1996; Wang et al., 1997a). However such a concept based on the assumption of a constant percolation velocity along bed depth was not fully justified until the measurements of the current work. More importantly, they did not formulate how to determine the frictional force between the liquid and packed bed.

As indicated in Eq. 3, to determine the liquid–particle frictional force it is necessary to know the liquid–particle friction factor, C_{DS}, and the specific liquid–particle contact area, a_{s-l}. For a continuous and saturated liquid flow in packed beds, estimates of C_{DS} and a_{s-l} have been well established (Yagi, 1993). In the case of the discrete and unsaturated liquid flow, however, it is extremely difficult to calculate the specific liquid–particle contact area due to the undetermined size of the liquid droplets or rivulets. In order to formulate the liquid–particle frictional force for discrete and unsaturated liquid flow in the packed bed, the average effective liquid diameter in the current model is assumed to be proportional to the effective capillary size in the packed bed, given by

$$d_l = \xi_1 \frac{\epsilon}{1-\epsilon} \phi d_p \tag{4}$$

Assuming that there are many individual liquid droplets or rivulets in the packed bed, the liquid–particle contact areas should be proportional to the total surface areas of the liquid. This implies the following correlation, that is,

$$a_{s-l} = \xi_2 \frac{1}{D_l} \tag{5}$$

where ϵ is the porosity of packed bed; ϕ is the particle shape factor; d_p is diameter of packing particles, mm; and ξ_1 and ξ_2 are proportionality constant, respectively.

Substituting Eqs. 2 to 5 into Eq. 1, and then letting $C'_{DS} = (\xi_2/\xi_1) C_{DS}$ gives

$$\rho_l g + \frac{C'_{DS}}{2} \frac{1-\epsilon}{\epsilon \phi d_p} \rho_l |u_l| u_l = 0 \tag{6}$$

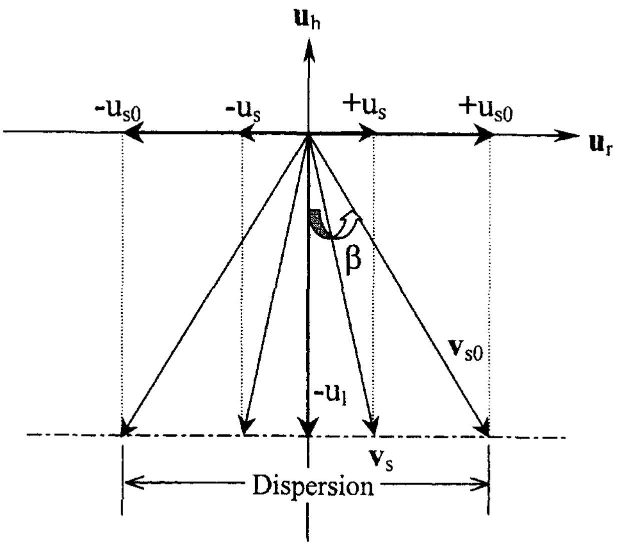

Figure 2. Stochastic dispersion of liquid flow in packed beds.

where the C'_{DS} can be defined as the modified liquid–particle friction factor, characterizing the interaction between the liquid and packing particles for discrete liquid flow through packed beds, C'_{DS} can only be determined with experimental measurements at the current stage.

In addition, the percolation flow of liquid in packed beds is not determined solely by the preceding force balance, but is also subject to stochastic motion. The stochastic motion of liquid, caused directly by liquid–particle interaction, leads to dispersion of the liquid within a well-defined region in the packed bed. This motion can be described using the stochastic model proposed in the previous studies (Wang et al., 1997a, b), in which a stochastic velocity is assumed to be normal to the major stream determined by the force-balance model. However, the stochastic velocity involved in this model has not been predicted yet, which makes its general application difficult.

Figure 2 illustrates conceptually the liquid dispersion due to stochastic motion. For percolation in packed beds, the direction of the major stream for the liquid flow always follows gravity. In this case, a horizontal velocity, u_s, will act on the liquid throughout the liquid percolation. This velocity combines with the percolation velocity, u_l, giving a compound velocity, v_l, which causes the dispersion of the liquid flow. The difference is that the velocity, u_s, is stochastic, probably due to the random pore geometry formed by the packing particles. Thus, a maximum stochastic velocity, u_{s0}, which dominates the maximum dispersion angle, β, exists. The stochastic motion will occur and can only occur within the flow region defined by the angles $\pm \beta$.

Two important process parameters C'_{DS} and β, can be used to model the discrete liquid percolation through a packed bed for an engineering application. To determine C'_{DS}, rearranging Eq. 6 gives

$$C'_{DS} = \frac{2 \epsilon \phi d_p g}{(1-\epsilon)|u_l|^2} \tag{7}$$

where the items on the righthand side of Eq. 7 are determined from experimental data.

For saturated flow, the liquid–solid friction factor varies with the liquid Reynolds number. We propose a similar relationship for unsaturated flow, as

$$C'_{DS} = f(\boldsymbol{Re}_l), \quad \text{where} \quad \boldsymbol{Re}_l = \frac{\rho_l u_l \phi d_p}{\mu_l} \tag{8a}$$

The Ergun equation for saturated flow is of the form

$$C'_{DS} = \frac{A}{\boldsymbol{Re}_l} + B \tag{8b}$$

A similar relationship for unsaturated flow is expected. The Ergun-type equation may not be the best-fit equation for unsaturated flow, but it has a clear physical significance. The first and second items on the right side of the Eq. 8b are the viscous and inertial friction contributor, respectively, where A and B are coefficients that can be determined experimentally.

The current work also attempts to determine the stochastic velocity based on the liquid dispersion experiments. Clearly, it is difficult to measure the stochastic velocity directly. As shown in Figure 2, however, the maximum stochastic velocity can be represented by the maximum dispersion angle, that is,

$$|\boldsymbol{u}_{s0}| = |\boldsymbol{u}_l| \tan\beta \tag{9a}$$

or

$$u_{s0} = u_1 \tan\beta \tag{9b}$$

Equation 9b gives a practical method for extracting the stochastic velocity from the experimental measurements of the percolation velocity and the maximum dispersion angle. To measure the maximum dispersion angle, it is necessary to measure the flowing boundary during the liquid percolation in the packed bed. Based on the measured boundary of the liquid flow, the maximum dispersion angle can be determined in the manner shown in Figure 3, given by

$$\beta = 90 - \tan^{-1}\left(\frac{dh}{dr}\right)\Bigg|_{r=0} \tag{10}$$

where curve $h = f(r)$ represents the best-fitted curve using the experimental data related to the measured boundary of the liquid flow region and r is the radial distance from the center (dispersion radius), m. A detailed description on the determination of the maximum dispersion angle using such a method can be found elsewhere (Wang et al., 1997c).

Results and Discussion

Liquid percolation through packed beds

Experiments were performed in beds of wax spheres. The effects of particle size (9, 15 and 19.4 mm), bed depth, and liquid flow rate on liquid percolation velocity were investigated for six liquids with a range of density, viscosity, and surface properties.

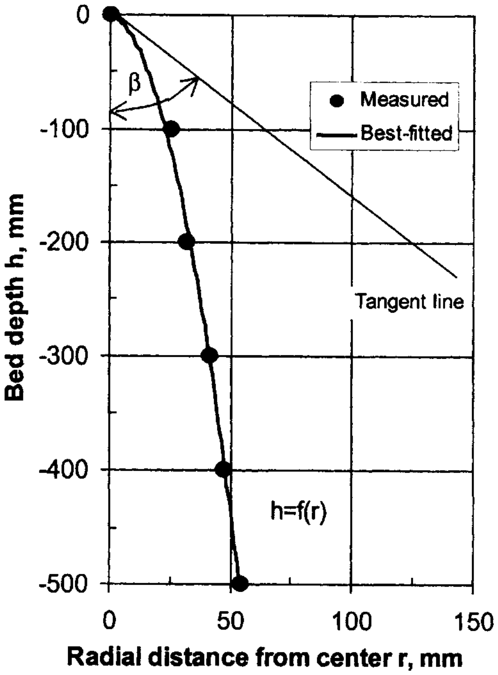

Figure 3. Determination of maximum dispersion angle for liquid percolation in packed beds.

Most previous model, simulation, or experimental studies used the superficial velocity to represent the velocity term for the saturated or unsaturated liquid flow. However, for an unsaturated liquid flow, the superficial velocity is a poor representation of the liquid flow behavior, so the actual velocity of the liquid flow has to be used. The liquid percolation velocity is considered to be the actual liquid velocity, described either by the maximum or the mean, as show in Figures 4 to 6, under various conditions.

Figure 4 shows the percolation velocity to be independent on the bed depth, with the experimental errors of less than 10% for maximum and 3% for mean. This result suggests that there is a constant percolation velocity for the unsaturated percolation flow in the packed bed. As indicated in ear-

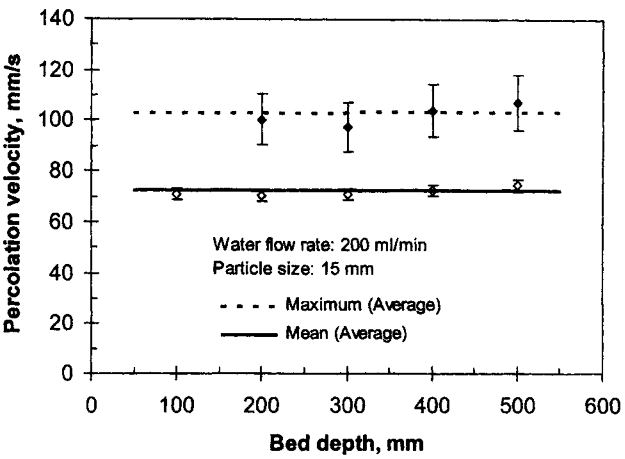

Figure 4. Percolation velocity of liquid in an unsaturated packed bed.

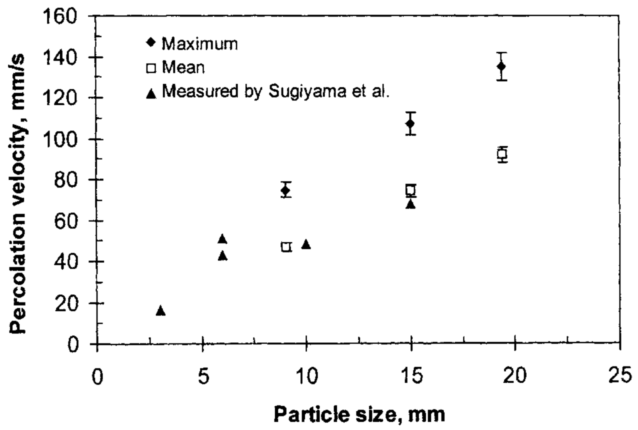

Figure 5. Effect of particle size on percolation velocity of water flowing through a bed of 500 mm depth at a flow rate of 200 mL/min.

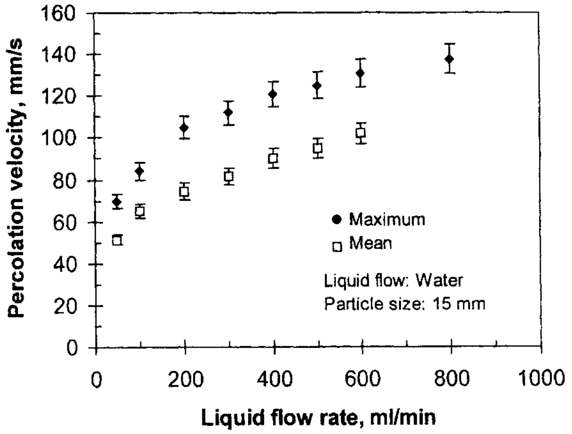

Figure 6. Change of percolation velocity under various liquid flow rates.

lier visual observations (Liu et al., 1997), the liquid flows as rivulets and droplets that cascade over the particles and are continuously breaking up and reforming to carry out momentum transfer. From a macroscopic view, this momentum transfer is a steady-state process. The gravity force of liquid rivulets or droplets and friction force between liquid and particles quickly come into balance so that a steady percolation velocity can be reached. This also provides evidence for the force-balance approach (Gupta et al., 1997; Wang et al., 1997a, b), in which initial acceleration from the point source of the liquid rivulets and droplets has been neglected at the macroscopic level.

Figure 5 illustrates the effect of particle size on the liquid percolation velocity. Results using a 50% glycerol–water solution in a similar experiment reported in the open literature (Sugiyama et al., 1987) are included for comparison. The result shows reasonable agreement in both the magnitude and the trend of the mean percolation velocity, with measurements reported in the literature. The liquid percolation velocity decreases as the particle size decreases, because the larger contact area leads to more frictional resistance between the liquid and particles.

The liquid flow rates also affect the percolation velocity, as shown in Figure 6. For the packed bed with a relatively large particle size (15 mm), the maximum and mean percolation velocities increase with increasing liquid flow rates. The percolation velocity increases dramatically in the flow-rate range of 0 to 150 mL/min, and then the rate of increase is slower at larger flow rates. The experimental observation indicates that the liquid flow pattern is also changed from "droplet" to "rivulet" (Liu et al., 1997) as the liquid flow rates increase. The percolation velocity of the droplets is slower than the rivulets. If a droplet size is too small to move, the the liquid will stay between the particles and waiting for the forthcoming liquid to reform into a large, moveable droplet. This process leads to a longer traveling time through the packed bed. On the other hand, liquid as rivulets continuously moves within the packed bed.

Similar experiments attempted with a 50% glycerol–water solution in the packed bed with 3-mm and 5-mm particles (Sugiyama et al., 1987) found the mean percolation velocity to be almost independent of the liquid flow rates for a packed bed of 3-mm particles. In a packed bed with small particles, liquid flow is more likely to completely fill the voids between the particles and form local saturated flow so that liquid flow rates have only a very minor effect on the liquid percolation velocity. However, for a packed bed of 5-mm particles, the percolation velocity slightly increased with an increase in the liquid flow rate above 150 mL/min.

Flow pattern and stochastic dispersion

These experiments were designed to investigate the effects of changing the flow pattern of the liquid percolation through packed beds by changing the bed depth and the particle size, respectively. The typical flow pattern is shown in Figures 7 and 8, in terms of the liquid flux mass velocity, mg/cm^{2}s.

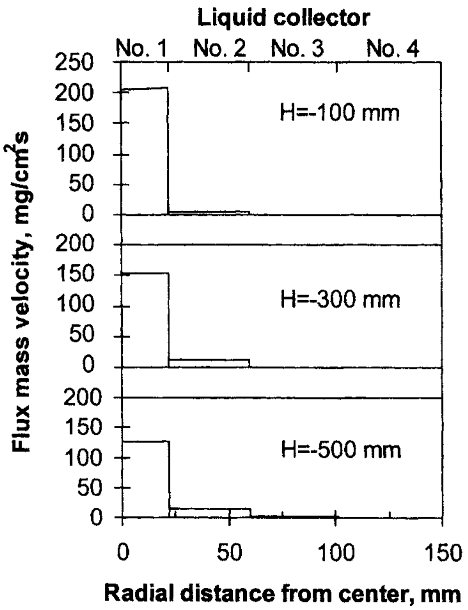

Figure 7. Distribution of flux mass velocity at different bed depths.

Water flowing through a bed of 15-mm particles at 200 mL/min flow rate.

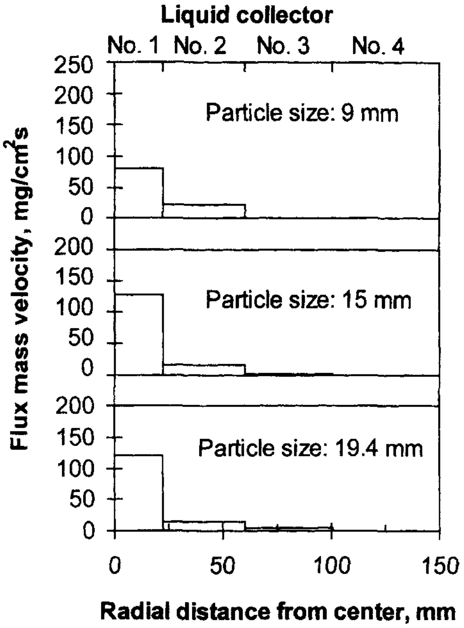

Figure 8. Influence of particle size on distribution of flux mass velocity.

Water flowing through a bed of 500 mm depth at 200 mL/min flow rate.

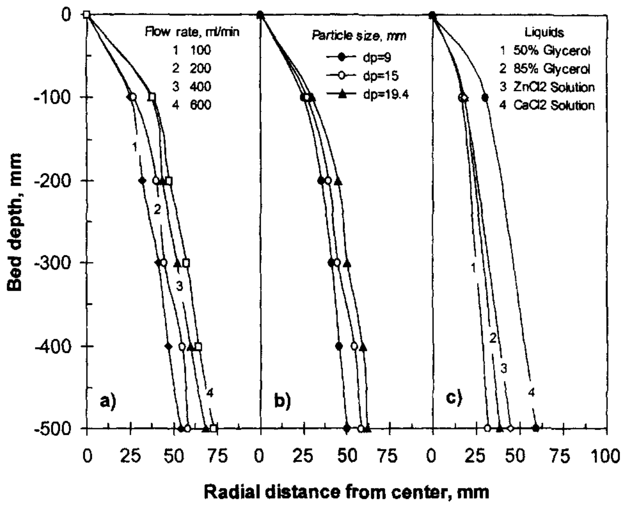

Figure 9. Flow boundary of liquid percolation in packed beds under various conditions

a) Particle size = 15 mm; (b) water flow rate = 200 mL/min; and (c) particle size = 15 mm and liquid flow rate = 200 mL/min.

Figure 7 shows the experimental measurements of liquid distribution over the cross section of uniform packing with a 15-mm wax sphere. The liquid distribution in the top part of the packed layer is more concentrated in the center region. For example, at a 100-mm bed depth, 89% of the total liquid is placed in the center annular collector, and only 11% is fed to the adjoined collector. Liquid distributions decrease in the center collector and increase in the outer collectors when liquid descends along the bed depths. Figure 8 shows similar radial profiles for three different particle sizes in a uniform packed bed with a bed depth of 500 mm. In this case, liquid distribution within the inner collector tends to decrease as the particle size decreases. The experimental observations agree with Sugiyama's (1987) experimental results. Resolution of the results is limited, as only three annular sections were used. However, the results were reproducible to within ±5%.

As noted in previous studies (Gupta et al., 1996; Liu et al., 1997), liquid stochastic dispersion is an important feature for the unsaturated percolation of liquid through a packed bed. The liquid stochastic dispersion is the lateral dispersion of the liquid due to stochastic interaction between the droplets or rivulets and particles. This implies that the liquid droplet or rivulet flow through the packed bed is controlled not only by the gravity itself, but also by the complex pore geometry formed by the packing particles. During the percolation flow, liquid–particle interaction occurs at a microscopic level, causing changes in the flow direction. Basically, the changes are stochastic, leading to dispersion within a certain flow region. The dispersion has been characterized, at a macroscopic level, by measuring the boundary of the liquid flow region on the various cross sections of a packed bed in the current study, as shown in Figure 9.

Figure 9a shows the measured flowing boundaries for the liquid dispersion in a 15-mm wax-sphere packed bed under the flow rates of 100 mL/min, 200 mL/min, 400 mL/min, and 600 mL/min water. It can be seen that the dispersion radius of a given cross section increases with increasing liquid flow rates. This is because an increasing liquid flow rate increases liquid mass per unit volume bed, strengthening the liquid momentum transfer. For the mass balance in the packed bed, an increase in liquid mass forces the liquid to spread to a farther boundary of the wet zone.

Figure 9b illustrates the effect of particle size on the boundary of the liquid (water) flow along the bed depth with a flow rate of 200 mL/min. In general, the larger the particle size, the wider the radial spreading of the liquid, and the further the liquid boundary line. This experimental result is consistent with the liquid distributions for different particle sizes, as shown in Figure 8.

The effect of liquid properties on the flowing boundary was investigated using 50% glycerol, 85% glycerol, and $ZnCl_2$ and $CaCl_2$ solutions, respectively. The liquid flow rates used were 200 mL/min. The 85% glycerol solution has the smallest wet zone, while the wet zone of the $CaCl_2$ solution is the largest (see Figure 9c). This experimental result also confirms that the physical properties of liquids do significantly affect liquid dispersion and boundary.

Liquid–particle interaction and dispersion performance

Table 2 summarizes the measurements of the mean percolation velocity and maximum dispersion angle for unsaturated liquid percolation in packed beds under the given experimental conditions. The modified liquid–particle friction factor, C'_{DS} can be calculated using Eqs. 7 from these measurements. Plotting the C'_{DS} against Re_l generates Figure 10, in which the experimental data are fitted by applying the least-square method to the proposed correlation defined by

Table 2. The Measured Mean Percolation Velocity and Maximum Dispersion Angle.

Liquid	Particle size (mm)	Porosity	Flow Rate (mL/min)	Percolation Velocity (m/s)	Dispersion angle, (deg)
Water	15	0.40	100	0.065	26
Water	9	0.36	200	0.047	32
Water	15	0.40	200	0.068	24
Water	19.4	0.42	200	0.092	23
0.5 glycerol	9	0.36	200	0.030	—
0.8 glycerol	9	0.36	200	0.021	—
0.85 glycerol	9	0.36	200	0.016	—
$CaCl_2$ solution	9	0.36	200	0.052	—
$ZnCl_2$ solution	9	0.36	200	0.025	—
0.5 glycerol	15	0.40	200	0.064	28
0.8 glycerol	15	0.40	200	0.053	27
0.85 glycerol	15	0.40	200	0.037	27
$CaCl_2$ solution	15	0.40	200	0.082	33
$ZnCl_2$ solution	15	0.40	200	0.053	31
0.5 glycerol	19.4	0.42	200	0.068	—
0.8 glycerol	19.4	0.42	200	0.054	—
0.85 glycerol	19.4	0.42	200	0.049	—
$CaCl_2$ solution	19.4	0.42	200	0.109	—
$ZnCl_2$ solution	19.4	0.42	200	0.081	—
Water	15	0.40	400	0.090	25
Water	15	0.40	600	0.102	28

Eq. 8b, giving

$$C'_{DS} = \frac{541}{Re_l} + 33 \tag{11}$$

Thus the liquid–particle interaction can be quantified using the modified friction factor, C'_{DS}. For instance, liquid flow in the lower part of the blast furnace is usually considered as inertial flow. The modified friction factor for this particular flow is essentially constant based on Eq. 11 at $C'_{DS} = 33 \pm 2$.

Although Eq. 11 has the same general form as the Ergun equation for saturated flow, the constants in the equation are quite different. The equivalent inertial constant for the saturated flow is 3.5 for the Ergun equation, compared to 33 in this case. Thus, models developed for the saturated flow lead to significant error when applied to unsaturated flow.

Figure 10 also implies that there is an obvious difference between saturated and unsaturated flow. For a saturated flow system, liquid flow usually can be controlled by superficial velocity. Physical liquid properties and contact angle can have a minor effect on the liquid–solid friction factor. However, an unsaturated flow is much more complex. Nevertheless, a relatively simple macroscopic correlation, as shown in Eq. 11, gives a good description of the effect of the liquid and particle properties. However, the effect of liquid flow rate, giving the transition from droplet to rivulet flow, is not covered in the correlation.

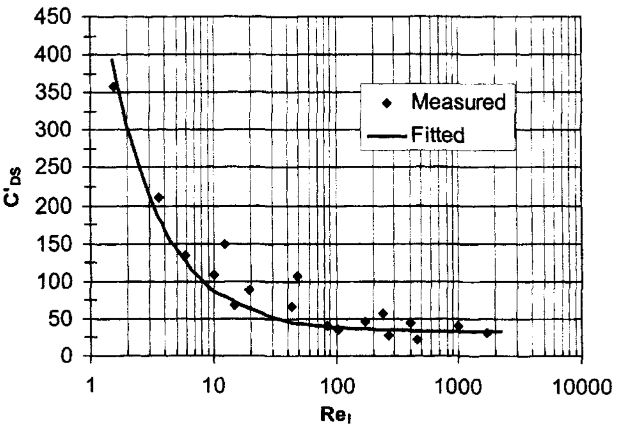

Figure 10. Estimation of liquid–particle friction factor.

The maximum dispersion angle determines the flow region for liquid percolation in an unsaturated bed. After referring to the empirical equation of liquid dynamic holdup proposed by Sugiyama et al. (1987), the liquid maximum dispersion angle was also assumed to be influenced by gravitational, surface, solid–liquid interfacial, inertial, and viscous force. These forces can be correlated with dimensionless group numbers such as Re_l, Ga_l, Cp, and N_c, where Re_l is the liquid Reynolds number and represents the ratio of inertial force to viscous force; Ga_l, the liquid Galileo number, is the ratio between the product of inertial force and gravitational force, and the square of viscous force; and Cp and Nc are the capillary number and dimensionless interfacial force of liquid, respectively. These dimensionless group numbers can be determined by the liquid properties and bed structure. For example, Re_l can be calculated using Eq. 8a, and Ga_l, Cp, and Nc are defined as follows

$$Ga_l = \frac{\rho_l^2 g(\phi d_p)^3}{\mu_l^2}$$

$$Cp = \frac{\rho_l g(\phi d_p)^2}{\sigma}$$

$$Nc = 1 + \cos(\theta)$$

where σ is the surface tension of the liquid, kg/s^2; and θ is the contact angle between the liquid and the particle material (wax).

It is therefore possible that the maximum dispersion angle can be empirically formulated as a function of the liquid properties and bed structure. By interpreting the experimental measurements, as shown in Table 2, into the four dimensionless group numbers just mentioned, an empirical equation was proposed for estimating the maximum dispersion angle, that is

$$\tan\beta = 2.95\boldsymbol{Re}_l^{0.31}\boldsymbol{Ga}_l^{-0.20}\left(\frac{\boldsymbol{Cp}}{\boldsymbol{Nc}}\right)^{-0.16}. \tag{12}$$

The result shown in Eq. 12 implies that the decreased gravitational force or increased liquid–particle interfacial forces and inertial force will increase dispersion. Increasing the viscous force also enhances liquid dispersion, but its effect is very limited compared with other forces.

Equation 12 should be considered as a preliminary correlation only, as the maximum dispersion angle and some of the expected controlling groups have varied over small ranges only. Nevertheless, the experimental variations measured here show a doubling of flow diameter (four times the flow area) as a result of the changing liquid properties. Such a variation can affect substantially the calculated holdup, and mass and heat transfer rates in a packed-bed reactor. Further work on the measurement and simulation of the stochastic behavior of unsaturated liquid flow is needed.

Conclusions

The unsaturated flow of liquid through an unsaturated packed bed can be quantified using a simple force balance with a stochastic dispersion component. The key parameters in this model are the liquid–particle friction factor and the maximum dispersion angle.

Unsaturated liquid flows are discrete in nature (either droplet or rivulet flow), and the actual percolation velocity, rather than the superficial velocity, should be used to characterize the flow. The percolation velocity did not vary with packed-bed depth, but was a strong function of liquid flow rate, liquid, and particle properties. The effects of liquid and particle properties (but not flow rate) are well captured by a simple, Ergun-style correlation between the liquid–particle friction factor and the Reynolds number, based on actual percolation velocity.

Liquid dispersion is characterized by the maximum dispersion angle. Liquid dispersion varies significantly with the liquid and particle properties. The tentative correlation suggested here needs further validation for a wider range of conditions.

Acknowledgments

The authors are grateful to the Australian Research Council and BHP Research for financial support. They are also grateful to Dr. V. Rudolph for helpful discussion.

Notation

a_{s-l} = specific liquid-particles contact area, m^{-1}
$\boldsymbol{Cp}$ = capillary number
C_{DS}, C'_{DS} = liquid–particle friction factor and modified liquid–particle friction factor
d_p, d_l = diameters of particles and liquid droplets or rivulets, respectively, m
F_g, F_l^s = gravitational force and frictional force between liquid and packed bed, N/m^3
$\boldsymbol{Ga}_l$ = liquid Galileo number
$\boldsymbol{g}$, g = unit gravity victor, and gravitational acceleration, m/s^2
h = depth of packed bed, m
$\boldsymbol{Nc}$ = dimensionless interfacial force
$\boldsymbol{Re}_l$ = liquid reynolds number
r = dispersion radius, m
$\boldsymbol{u}_l$, u_l = velocity vector and velocity of liquid percolation, m/s
$\boldsymbol{u}_{s0}$, u_{s0} = maximum velocity vector and velocity for stochastic dispersion, m/s
$\boldsymbol{u}_s$ = velocity vector for stochastic dispersion, m/s

Greek letters

β = maximum dispersion angle defined by Figures 2 and 3, deg
ϵ = porosity of packed bed
ϕ = shape factor of particles
μ_l = viscosity of liquid, kg/ms
θ = contact angle between liquid and particle material (wax), deg
ρ_l = density of liquid, kg/m^3
σ = surface tension of liquid, kg/s^2

Literature Cited

Apelian, D. and R. Mutharasan, "Filtration: A Melt Refining Method," *J. of Metals*, **32**, 14 (1980).

Austin, P. R., H. Nogami, and J. Yagi, "A Mathematical Model of Four Phase Motion and Heat Transfer in the Blast Furnace," *ISIJ Int., 37, 485(1997).*

Chew, S. J., G. X. Wang, A. B. Yu, and P. Zulli, "Experimental Study of Liquid Flow in the Blast Furnace Cohesive Zone," *Iron Steel Making*, **24**, 392 (1997).

Eto, Y., K. Takeda, S. Miyagawa, S. Taguchi, and H. Itaya, "Experiments and Simulation of the Liquid Flow in the Dropping Zone," *ISIJ Int.*, **33**, 681 (1993).

Frisvold, F., T. A. Engh, S. T. Johansen, and T. Pedersen, "Removal of Inclusions—A Survey and Comparison of Principles," *Light Metals*, 1125 (1992).

Gupta, G. S., J. D. Litster, V. R. Rudolph, E. T. White, and A. Domanti, "Model Studies of Liquid Flow in the Blast Furnace Lower Zone," *ISIJ Int.*, **36**, 32 (1996).

Gupta, G. S., J. D. Litster, E. T. White, and V. R. Rudolph, "No-Wetting Flow of a Liquid Through a Packed Bed with Gas Cross-Flow," *Met. Trans.*, **28B**, 579 (1997).

Kolb, W. B., T. R. Melli, J. M. d. Santos, and L. E. Scriven, "Cocurrent Downflow in Packed Beds—Flow Regimes and Their Acoustic Signatures," *Ind. Eng. Chem. Res.*, **29**, 2381(1990).

Liu, D. Y., S. Wijeratne, and J. D. Litster, "Visualization and Maximum Percolation Velocity of Non-Wetting Liquid Flow Through a 2-D Packed Bed," *Scand. J. Met.*, **26**, 79 (1997).

Macdonald, I. F., M. S. El-Sayed, K. Mow, and F. A. L. Dullien, "Flow Through Porous Media—Ergun Equation Revisited," *Ind. Eng. Chem. Fundam.*, **18**, 199 (1979).

Melli, T. R., J. M. d. Santos, W. B. Kolb, and L. E. Scriven, "Cocurrent Downflow in Networks of Passages—Miscroscale Roots of Macroscale Flow Regimes," *Ind. Eng. Chem. Res.*, **29**, 2367 (1990).

Ohno, Y., and Kondo, K. "Investigation of Gas and Liquid Flow in the Lower Part of Blast Furnace by Mathematical Model," *Trans. Iron Steel Inst. Jpn.*, **20**, B495 (1980).

Ohno, Y., and M. Schneider, "Effect of Horizontal Gas Flow on Liquid Dropping Flow in Two-Dimensional Packed Bed," *Tetsu-to-Hagane*, **74**, 1923 (1988).

Payatakes, A. C., H. Y. Park, and J. Petrie, "A Visual Study of Particle Deposition and Reentrainment During Depth Filtration of Hydrosols with a Polyelectrolyte," *Chem. Eng. Sci.*, **36**, 1319 (1981).

Rode, S., N. Midoux, M. A. Latifi, and A. Storck, "Multiple Hydrodynamic States in Trickle Beds Operating in High-Interaction Regimes: Liquid Saturation and Flow Regime Transitions," *Chem. Eng. Sci.*, **49**, 2535 (1994).

Sugiyama, T., A. Nakagawa, H. Shibaike, and Y. Oda, "Analysis on Liquid Flow in the Dropping Zone of Blast Furnace," *Tetsu-to-Hagane*, **73**, 2044 (1987).

Szekely, J., and Y. Kajiwara, "A Mathematical Representation of Spatially Non-Uniform, Counter-Current Flow of Gases and Liquids in Packed Beds," *Trans. Iron Steel Inst. Jpn.*, **19**, 76 (1979).

Wang, G. X., S. J. Chew, A. B. Yu, and P. Zulli, "Model Study of Liquid Flow in the Blast Furnace Lower Zone," *ISIJ Int.*, **37**, 573 (1997a).

Wang, G. X., S. J. Chew, A. B. Yu, and P. Zulli, "Modelling the Discontinuous Liquid Flow in a Blast Furnace," *Met. Trans.*, **28B**, 333 (1997b).

Wang, G. X., D. Y. Liu, J. D. Litster, A. B. Yu, S. J. Chew, and P. Zulli, "Experimental and Numerical Simulation of Liquid Flow in a Packed Bed," *Chem. Eng. Sci.*, **52**, 4013 (1997c).

Wang, J., R. Takahashi, and J. Yagi, "Simulation Model of the Gas-Liquid Flows in the Packed Bed," *Tetsu-to-Hagane*, **77**, 1585 (1991).

Yagi, J., "Mathematical Modelling of the Flow of Four Fluids in a Packed Bed," *ISIJ Int.*, **33**, 703 (1993).

Zimmerman, S. P., and K. M. Ng, "Liquid Distribution in Trickling Flow Trickle-Bed Reactors," *Chem. Eng. Sci.*, **41**, 861(1986).

Manuscript received Apr. 17, 2000, and revision received Oct. 23, 2001.